JACS ARTICLES

Published on Web 12/31/2009

Synthesis of Dispersible Pd@CeO_2 Core−Shell Nanostructures by Self-Assembly

Matteo Cargnello,[†,‡] Noah L. Wieder,[†] Tiziano Montini,[‡] Raymond J. Gorte,*[,†] and Paolo Fornasiero*[,‡]

Department of Chemical and Biomolecular Engineering, University of Pennsylvania, 311A Towne Building, 220 South 33rd Street, Philadelphia, Pennsylvania 19104, and Chemistry Department, ICCOM-CNR, INSTM, Center of Excellence for Nanostructured Materials (CENMAT), University of Trieste, via L. Giorgieri 1, 34127 Trieste, Italy

Received October 27, 2009; E-mail: gorte@seas.upenn.edu; pfornasiero@units.it

Abstract: A methodology is described for the preparation of Pd@CeO_2 core−shell nanostructures that are easily dispersible in common organic solvents. The method involves the synthesis of Pd nanoparticles protected by a monolayer of 11-mercaptoundecanoic acid (MUA). The carboxylic groups on the nanoparticle surfaces are used to direct the self-assembly of a cerium(IV) alkoxide around the metal particles, followed by the controlled hydrolysis to form CeO_2. The characterization of the nanostructures by means of different techniques, in particular by electron microscopy, allowed us to demonstrate the nature of core−shell systems, with CeO_2 nanocrystals forming a shell around the MUA-protected Pd core. Finally, an example of the use of these nanostructures as flexible precursors for the preparation of heterogeneous catalysts is reported by investigating the reactivity of Pd@CeO_2/Al_2O_3 nanocomposites toward CO oxidation, water−gas shift (WGS), and methanol steam reforming reactions. Together with CO adsorption data, these observations suggest the accessibility of the Pd phase in the nanocomposites.

1. Introduction

The ability to design and prepare materials with atomic scale accuracy is of significant importance to gain new materials properties. This has been demonstrated for applications in nanoparticle arrays,[1] organic semiconductors for spintronic devices,[2] semiconductor nanocrystals,[3] carbon nanotubes,[4] and functional open-frameworks.[5] In this context, the increasing interest in core−shell structures is due to the possibilities for new physical and chemical characteristics, often different and improved from those of the constituent components. This opens new opportunities for their successful application in various fields like catalysis, optoelectronics, separation technology, coatings, and additives.[6] The preparation of such composites is still a matter of intensive study, mainly due to the need for better control of the characteristics of the resulting materials, their compositions, and properties.

One primary challenge involves the tailored coating of particles with the desired organic, inorganic, or bioorganic layer. A well-established example of this is the coating of quantum dots or nanoparticles with polymers or other organic molecules.[7,8] The use of inorganic coatings is less developed and mostly limited to the use of SiO_2.[9−11] The reasons for working with SiO_2 are the chemical inertness, optical transparency, and high-temperature stability of the silica films, together with the well-known chemistry of its precursors (e.g., tetraethylorthosilicate, TEOS). Moreover, there are some recent examples of using ZrO_2,[12] SnO_2,[13] and other less-inert inorganic shells for the preparation of core−shell systems in high-temperature catalytic applications. Core−shell structures composed of platinum and gold particles embedded into CeO_2 have been made[14,15] using a microemulsion approach and have proven to be active heterogeneous catalysts. In addition to requiring many slow steps, the microemulsion method cannot produce materials that can be easily dispersed onto supports.

Among the inorganic shells that have been studied, ceria is of special interest because it is an essential component in some important applications.[16] In catalysis, the relative ease with which Ce shuttles between III and IV oxidation states leads to enhanced oxidation reaction rates[17,18] and water−gas shift

[†] University of Pennsylvania.
[‡] University of Trieste.

(1) Talapin, D. V.; Shevchenko, E. V.; Bodnarchuk, M. I.; Ye, X.; Chen, J.; Murray, C. B. *Nature* **2009**, *461*, 964.
(2) Dediu, V. A.; Hueso, L. E.; Bergenti, I.; Taliani, C. *Nat. Mater.* **2009**, *8*, 707.
(3) Reiss, P.; Protière, M.; Li, L. *Small* **2009**, *5*, 154.
(4) Avouris, P.; Freitag, M.; Perebeinos, V. *Nat. Photon.* **2008**, *2*, 341.
(5) Natarajan, S.; Mandal, S. *Angew. Chem., Int. Ed.* **2008**, *47*, 4798.
(6) Caruso, F. *Adv. Mater.* **2001**, *13*, 11.
(7) Daniel, M. C.; Astruc, D. *Chem. Rev.* **2004**, *104*, 293.
(8) Ahmadi, T. S.; Wang, Z. L.; Green, T. C.; Henglein, A.; El-Sayed, M. A. *Science* **1996**, *272*, 1924.
(9) Liz-Marzán, L. M.; Giersig, M.; Mulvaney, P. *Langmuir* **1996**, *12*, 4329.
(10) Budroni, G.; Corma, A. *Angew. Chem., Int. Ed.* **2006**, *45*, 3328.
(11) Park, J. N.; Forman, A. J.; Tang, W.; Cheng, J.; Hu, Y. S.; Lin, H.; McFarland, E. W. *Small* **2008**, *4*, 1694.
(12) Arnal, P. M.; Comotti, M.; Schüth, F. *Angew. Chem., Int. Ed.* **2006**, *45*, 8224.
(13) Yu, K.; Wu, Z.; Zhao, Q.; Li, B.; Xie, Y. *J. Phys. Chem. C* **2008**, *112*, 2244.
(14) Yeung, C. M. Y.; Yu, K. M. K.; Fu, Q. J.; Thompsett, D.; Petch, M. I.; Tsang, S. C. *J. Am. Chem. Soc.* **2005**, *127*, 18010.
(15) Yeung, C. M. Y.; Tsang, S. C. *J. Phys. Chem. C* **2009**, *113*, 6074.
(16) Trovarelli, A. *Catal. Rev.* **1996**, *38*, 439.
(17) Abad, A.; Concepción, P.; Corma, A.; García, H. *Angew. Chem., Int. Ed.* **2005**, *44*, 4066.

 10.1021/ja909131k

activity.[19] Inorganic Ce compounds have also been used in light shielding and window materials because of their ability to absorb UV light.[20] Because of these properties, the preparation of metal-core/ceria-shell structures is potentially of great importance.

The dispersibility of oxide nanoparticles and core−shell structures with oxide shells is a key property for avoiding formation of aggregates. While nanometer-scale, silica-based systems may be soluble in water or other polar solvents by employing functionalized silicon alkoxides,[21] this approach to dispersibility is less easily applicable to other oxides. A more general method for dispersing SiO_2 and other oxides in either polar or nonpolar solvents involves the use of surfactants or capping ligands at the external surface.[22] However, this method does not allow a fine-tuning of the dimensions of either the metal core or the shell thickness.

Although there have been several reports of methods to prepare ceria particles that are dispersible in organic solvents,[23−26] we are unaware of preparation procedures for dispersible core−shell structures involving ceria-encapsulated metal nanoparticles (M@CeO_2). In particular, dispersible ceria-encapsulated Pd has not been reported to date, although this system is very interesting for its numerous applications especially in catalysis. One of the main problems is that functionalized cerium precursors such as alkoxides are not as available as those of silicon. A solution is represented by the use of functionalized Pd nanoparticles with appropriate groups exposed on the surface of the organic passivating monolayer.

Our strategy involved first the preparation of Pd nanoparticles that present carboxylic groups on the surface, because carboxylates have a high affinity for Ce(IV) species. However, the synthesis of carboxylate-functionalized metal nanoparticles is not trivial because carboxylates are not always compatible with nanoparticle synthesis conditions. For instance, the use of the common reducing agent $NaBH_4$ is potentially problematic, given the presence of carboxylic groups on the particles. To enhance functional group tolerance of the synthesis, a single-step procedure was reported using the mild reducing agent 9-borabicyclo[3.3.1]nonane (9-BBN) for the preparation of Au nanoparticles protected by 11-mercaptoundecanoic acid (MUA) and other functional thiol ligands.[27] This approach was extended to Pd nanoparticles but only using alkyl thiols, and the average dimension of the particles in this study was greater than 2.5 nm. Thiol exchange, whereby a nonfunctionalized thiol ligand is exchanged for a functionalized thiol, is another method reported in the literature that allows the introduction of complex functionalities that are incompatible with the synthetic conditions.[28] This approach is limited in that complete exchange with the functionalized thiol is difficult and time-consuming, because the reaction involves an equilibrium process that must be driven to completion. The exchange of thiols onto particles passivated with more weakly bound protecting agents (e.g., polymers, amines, carboxylic acids) is a potential alternative due to the higher stability of the S−Pd bond. However, the use of weaker passivating ligands for nanoparticle synthesis generally leads to large metal particles. In general, the use of thiols as passivating agents during nanoparticle synthesis is advantageous due to the possibility to obtain very small and monodisperse nanoparticles.[28] To date, a direct method to obtain small and monodisperse thiol-protected Pd nanoparticles with carboxylic groups on the surface is still unavailable.

Here, we report a route to obtain dispersible Pd@CeO_2 core−shell nanostructures. We describe the preorganization in solution of the parts, which leads to Pd@CeO_2 core−shell nanostructures that are dispersible in nonpolar and weakly polar solvents, including THF, dichloromethane, toluene, and hexane. Our strategy exploits monolayer-protected Pd nanoparticles (PdNPs), functionalized with carboxylic groups, and cerium alkoxides as building blocks. The synthesis is highly flexible and allows changes in the dimensions of the metal core, the thickness of the ceria surrounding layer, and the dispersibility of the product in nonpolar solvents. Examples of using these nanostructures as precursors for catalysts for CO oxidation, the water−gas shift, and methanol steam reforming reactions are reported. In addition, CO adsorption data corroborate the fact that the Pd phase in the Pd@CeO_2 core−shell nanostructures is accessible.

2. Experimental Section

2.1. Materials. Potassium tetrachloropalladate(II) (32.04% as Pd) was purchased from ChemPur. Cerium ammonium nitrate ($(NH_4)_2Ce(NO_3)_6$, CAN, ≥98.5%), 11-mercaptoundecanoic acid (MUA, 95%), sodium methoxide (ca. 25 wt % in methanol), and dodecanoic acid (99% minimum) were purchased from Sigma-Aldrich. Sulfuric acid (95−97%), tetraoctylammonium bromide (TOABr, ≥98%), and $Pd(NO_3)_2 \cdot 2H_2O$ (~40% as Pd) were purchased from Fluka. 1-Decanol (98+%) was purchased from Alfa Aesar, and $NaBH_4$ (98+%) was from Acros Organics. Al_2O_3 Puralox TH100/150 was purchased by Sasol and calcined at 900 °C for 24 h. Prior to being used, the Al_2O_3 was degassed under vacuum at 225 °C overnight. All of the solvents were of reagent grade and used as received, except those used for the preparation of cerium(IV) tetrakis(decyloxide). The solvents used in the preparation of this compound were stored over activated 3 Å molecular sieves overnight prior to use. Deuterated solvents were purchased from Aldrich and used as received.

2.2. Synthesis of MUA-Pd Nanoparticles. The synthesis of MUA-Pd nanoparticles was adapted from a literature method.[28] A typical synthesis started with the transfer of the $PdCl_4^{2-}$ anion, obtained by dissolving K_2PdCl_4 (25.8 mg, 0.079 mmol) in water (5 mL), to dichloromethane (15 mL) using TOABr (64.9 mg, 0.119 mmol, 1.5 mol vs Pd) as the transferring agent. The aqueous phase was discarded, and acetone (15 mL) was added. 11-Mercaptoundecanoic acid (MUA, 9.1 mg, 0.040 mmol, 0.5 mol vs Pd) was added first, followed by the addition of 10 mL of a methanolic solution (10 mL) of $NaBH_4$ (30.0 mg, 0.793 mmol, 10 mol vs Pd). The solution immediately turned from orange to black, suggesting the reduction of Pd(II) to Pd(0), and then formed a black, waxy precipitate. This precipitate was filtered on a glass frit and washed with excess acetone and methanol, after which the particles were recovered by dissolution in acidified THF (using 0.5 M methanolic H_2SO_4 solution). The black precipitate was completely soluble, indicating that the Pd nanoparticles were isolated within precipitate.

(18) Esch, F.; Fabris, S.; Zhou, L.; Montini, T.; Africh, C.; Fornasiero, P.; Comelli, G.; Rosei, R. *Science* **2005**, *309*, 752.
(19) (a) Hilaire, S.; Wang, X.; Luo, T.; Gorte, R. J.; Wagner, J. *Appl. Catal., A* **2001**, *215*, 271. (b) Cargnello, M.; Montini, T.; Polizzi, S.; Wieder, N. L.; Gorte, R. J.; Graziani, M.; Fornasiero, P. *Dalton Trans.* **2010**, in press, doi: 10.1039/b916035c.
(20) Tsunekawa, S.; Fukuda, T.; Kasuya, A. *J. Appl. Phys.* **2000**, *87*, 1318.
(21) Jana, N. R.; Earhart, C.; Ying, J. Y. *Chem. Mater.* **2007**, *19*, 5074.
(22) Qi, Y.; Chen, M.; Liang, S.; Zhao, J.; Yang, W. *Colloids Surf., A* **2007**, *302*, 383.
(23) Inoue, M.; Kimura, M.; Inui, T. *Chem. Commun.* **1999**, 957.
(24) Kar, S.; Patel, C.; Santra, S. *J. Phys. Chem. C* **2009**, *113*, 4862.
(25) Gu, H.; Soucek, M. D. *Chem. Mater.* **2007**, *19*, 1103.
(26) Depner, S. W.; Kort, K. R.; Jaye, C.; Fischer, D. A.; Banerjee, S. *J. Phys. Chem. C* **2009**, *113*, 14126.
(27) Sardar, R.; Shumaker-Parry, J. S. *Chem. Mater.* **2009**, *21*, 1167.
(28) Zamborini, F. P.; Gross, S. M.; Murray, R. W. *Langmuir* **2001**, *17*, 481.

^{1}H NMR (acetone-d_6) δ: 1.38 (br, $-CH_2-$), 1.62 (br, $-CH_2CH_2S$), 2.30 (br, $-CH_2COOH$). IR (KBr) ν (cm^{-1}): 2921, 2848, 1713, 1611, 1449, 1431, 1372, 1186, 858, 816, 600, 477. UV−vis (THF, $c = 0.025$ mM as Pd): monotonic decay from 300 nm. TEM: $d_m = 1.8$ nm; $\sigma = 0.2$ nm; $n = 165$.

2.3. Synthesis of Cerium(IV) Tetrakis(decyloxide). The preparation of cerium(IV) tetrakis(decyloxide) [$Ce(C_{10}H_{21}O)_4$, $Ce(OR)_4$] followed previously reported procedures[29,30] with slight modifications. Cerium ammonium nitrate (CAN) (5.00 g, 9.12 mmol) was dissolved in 50 mL of MeOH, after which 1-decanol (6.97 mL, 4 mol vs Ce) was added. Next, a 25 wt % solution of MeONa in MeOH (12.51 mL, 6 mol vs Ce) was introduced dropwise, causing formation of gaseous NH_3 and precipitation of a bright yellow solid (cerium(IV) methoxide) and a white solid ($NaNO_3$). The mixture was stirred for 1 h, before removing the solvent by evaporation to yield an orange-colored oil with $NaNO_3$ powder mixed in. The oil was dissolved into 25 mL aliquots of dichloromethane, and the solvent was evaporated again. This procedure was repeated twice. Finally, the compound was dissolved in DCM, the $NaNO_3$ was filtered out, and the solvent was removed by evaporation. The orange-oil product (7.00 g, 99%) was used without further purification.

^{1}H NMR ($CDCl_3$) δ: 0.88 (br, $-CH_3$), 1.28 (br, CH_2), 1.57 (br, $-CH_2CH_2O$), 3.67 (br, $-CH_2O$). IR (KBr) ν (cm^{-1}): 2954, 2921, 2851, 1465, 1368, 1074, 1053, 719.

2.4. Preparation of Pd@CeO_2 Nanostructures. The preparation of Pd@CeO_2 with the desired composition (Pd concentration of 2.5, 10, or 50 wt %) was achieved by adding the THF solution of MUA-Pd nanoparticles to the THF solution of cerium(IV) tetrakis(decyloxide), followed by the addition of a THF solution of dodecanoic acid. Typically, 10 mL of the THF solution of MUA-Pd nanoparticles was slowly added to 10 mL of the THF solution of cerium(IV) tetrakis(decyloxide), followed by the addition of dodecanoic acid (1 mol vs Ce) dissolved into 10 mL of THF. Hydrolysis of cerium(IV) alkoxide in the Pd−Ce solution was carried out by slowly (over a period of 4 h) adding up to 1.2 mL of H_2O (up to 120 mol vs Ce) dissolved in 10 mL of THF.

^{1}H NMR ($CDCl_3$) δ: 0.90 (br, $-CH_3$), 1.2−1.6 (br, CH_2). IR (KBr) ν (cm^{-1}): 2953, 2921, 2851, 1534, 1424, 562.

2.5. Preparation of Pd@CeO_2/Al_2O_3 Catalysts. Pd@CeO_2/Al_2O_3 catalysts were prepared using the Pd@CeO_2 nanostructures as the starting material. Pd(10 wt %)@CeO_2 nanostructures were synthesized as described in section 2.4 and dissolved in THF (50 mL). The appropriate mass of degassed Al_2O_3 was then added to the Pd@CeO_2 solution to achieve the nominal loading for Pd and CeO_2, 1 and 9 wt %, respectively. After the mixture was stirred overnight, THF was removed by evacuation, after which the powder was dried at 120 °C, crushed to particle sizes below 150 μm, and finally calcined at 500 °C for 5 h, using a heating rate of 3 °C min^{-1} to reach the calcination temperature.

2.6. Characterization Techniques. NMR spectra were recorded on a JEOL GX-400 MHz (operating at 400 MHz for ^{1}H) using $CDCl_3$ or acetone-d_6 as solvents. ^{1}H NMR spectra were referenced to the residual protons in the deuterated solvent. FT-IR spectra were recorded on a Perkin-Elmer FT-IR/Raman 2000 instrument in the transmission mode using KBr pellets of the sample. UV−visible spectra were recorded on a UV−vis Unicam Helios β spectrophotometer.

Specimens for transmission electron microscopy (TEM) were prepared by placing a single drop of the sample dissolved in THF onto a 200-mesh copper grid coated with an amorphous holey carbon film. The grid was then dried in air for 24 h. Images were obtained with a JEOL 2010F high-resolution field-emission microscope (1.7 nm point-to-point resolution), operating at 200 keV and equipped with a Gatan slow-scan CCD camera (mod. 794), X-ray energy dispersive spectroscopy (EDS, PGT-IMIX), and EELS (Gatan Imaging) used for energy filtered imaging. The latter technique is used to collect the electrons that have lost energy in a given range of the electron energy loss (EEL) spectrum, thus allowing one to discriminate in the sample the contributions from different elements. Elemental composition profiles of the samples were measured using EDS in scanning transmission electron microscopy (STEM) mode using a spot size of 25 nm. Damage or transformation of the samples was not observed under the experimental conditions during investigation.

Samples for atomic force miscroscopy (AFM) were prepared by placing a single drop of a very dilute solution of the prepared nanoparticles/nanostructures onto a cleaned YSZ(100) single crystal and then evaporating the solvent under a stream of dry nitrogen. Prior to deposition, the YSZ substrate was cleaned by immersion in piranha solution (conc. H_2SO_4 and 30% H_2O_2, 3:1) at room temperature for at least a half hour, followed by thorough rinsing in deionized H_2O, acetone, and finally by drying under a stream of nitrogen. All AFM measurements were performed on a Pacific Nanotechnology Nano-E AFM system operated in close-contact (tapping) mode.

The Pd dispersion was determined by CO adsorption. A fixed pretreatment procedure was used for the Pd@CeO_2/Al_2O_3 catalyst. Specifically, 0.3 g of catalyst was loaded into a sample cell and evacuated at 673 K. While the sample was held at 673 K, it was exposed to 200 Torr O_2 for several minutes, evacuated, and reexposed to 200 Torr O_2 and evacuated twice more. Afterward, the sample was cooled to 423 K and exposed to 200 Torr H_2 for several minutes to reduce the Pd and then evacuated at 423 K three times. To suppress the reaction of CO with ceria, the adsorption measurements were performed at 195 K by cooling the sample in a dry ice/acetone bath according to the procedure reported by Tanabe and co-workers.[31] CO uptake was determined by adding small pulses of CO until a rise in the pressure of the sample cell was detected.

2.7. Catalytic Tests. All catalytic tests were conducted at atmospheric pressure. The fresh samples were positioned in a U-shaped, quartz microreactor with internal diameter of 4 mm, and pretreated in a flowing mixture of 5% O_2−95% Ar at 40 mL min^{-1} for 30 min at 450 °C, after heating from room temperature at 10 °C min^{-1}. No other activation procedures (e.g., reduction) were performed. Liquid reagents were introduced in the reaction mixture by means of a syringe (Hamilton GASTIGHT) and an infusion pump (KNF mod. 2000).

For the CO oxidation, ∼38 mg of catalyst was used, and the total gas flow rate under reaction conditions was 48.0 mL min^{-1} to ensure a gas hourly space velocity (GHSV) of ∼75 000 mL g^{-1} h^{-1}. The feed gas was 1.0% CO and 4.0% O_2 diluted in Ar. The gaseous mixture was introduced into the reactor at room temperature, and the reactor was then heated to 150 °C at 2 °C min^{-1}.

For the water−gas shift reaction (WGSR), ∼43 mg of catalyst was used, and the total gas flow rate under reaction conditions was 54.3 mL min^{-1} to ensure a gas hourly space velocity (GHSV) of ∼75 000 mL g^{-1} h^{-1}. The feed gas was 3.0 vol % CO and 3.0 vol % H_2O, diluted in Ar. The gaseous mixture was introduced into the reactor at 250 °C, and the reactor was then heated to 400 °C at 2 °C min^{-1}.

For the methanol steam reforming reaction, ∼16 mg of catalyst was used, and the total gas flow rate under reaction conditions was 39.4 mL min^{-1} to ensure a gas hourly space velocity (GHSV) of ∼150 000 mL g^{-1} h^{-1}. The feed mixture was CH_3OH/H_2O 1: 4, diluted in Ar. The gaseous mixture was introduced into the reactor at 125 °C, and the reactor was then heated to 500 °C at 0.5 °C min^{-1}.

Reactants and products were analyzed using a mass spectrometer (Hyden Analytical HPR20) for WGS and CO oxidation reactions,

(29) Gradeff, P. S.; Schreiber, F. G.; Brooks, K. C.; Sievers, R. E. *Inorg. Chem.* **1985**, *24*, 1110.
(30) Chen, H.; Cronin, J. A.; Archer, R. D. *Inorg. Chem.* **1995**, *34*, 2306.
(31) Tanabe, T.; Nagai, Y.; Hirabayashi, T.; Takagi, N.; Dohmae, K.; Takahashi, N.; Matsumoto, S.; Shinjoh, H.; Kondo, J. N.; Schouten, J. C.; Brongersma, H. H. *Appl. Catal., A* **2009**, *370*, 108.

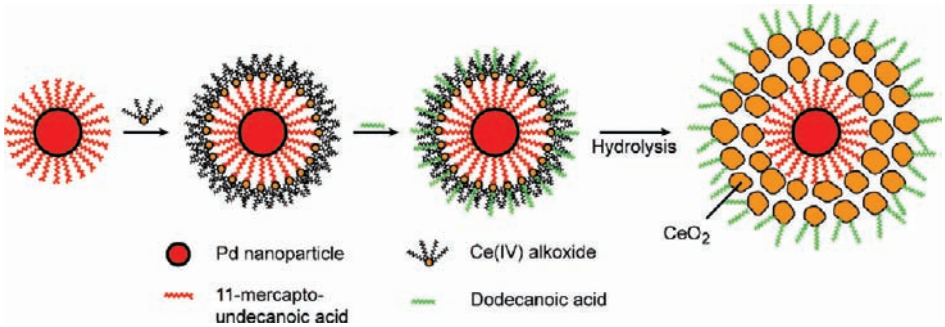

Figure 1. Schematic representation of the procedure to obtain dispersible Pd@CeO_2 core−shell nanostructures.

and with a GC chromatograph (HP 5890) equipped with TCD and FID detectors for the methanol steam reforming reaction. Conversions and yields were calculated as reported in the Supporting Information (p S7).

3. Results and Discussion

3.1. Strategy for Synthesis. Our synthesis procedure for Pd@CeO_2 nanostructures consists of the following three steps, shown schematically in Figure 1: (1) the synthesis of thiolate-protected Pd nanoparticles using 11-mercaptoundecanoic acid (MUA) as the passivating agent; (2) the self-assembly of cerium(IV) tetrakis(decyloxide) on protected Pd nanoparticles and its modification by means of dodecanoic acid; and (3) the hydrolysis under controlled conditions of the remaining alkoxy groups bound to Ce atoms to obtain dispersible Pd@CeO_2 nanostructures.

3.2. Synthesis of MUA-Pd Nanoparticles. It is important to recognize that it was essential to achieve a very high density of carboxylic groups on the surface of the particles to successfully synthesize the dispersible Pd@CeO_2 nanostructures. Consistent with this, the use of a mixed monolayer[10] resulted in the formation of agglomerates when the hydrolysis process was carried out. Therefore, particular attention was given to the synthesis of MUA-protected Pd nanoparticles.

The MUA-protected particles were synthesized modifying a literature procedure that involves the transfer of $PdCl_4^{2-}$ ions into the organic phase using TOABr as the phase transfer agent. The choice of solvent mixture during the preparation (1:1 acetone and dichloromethane) was critical for keeping the intermediate Pd−thiol complex in solution prior to reduction with $NaBH_4$, because the complex was observed to precipitate when toluene or pure dichloromethane was used. The addition of $NaBH_4$ causes rapid agglomeration of the particles in the form of flakes. This phenomenon, induced by the basic reaction media, was used to purify the desired product from unreacted compounds and/or byproducts.[32] Kimura and co-workers previously reported a similar scheme whereby base-induced agglomeration was exploited to purify carboxylate-functionalized gold nanoparticles.[32] Indeed, we found that the agglomerated particles could be efficiently recovered by filtration, followed by washing, redissolution in THF, and then treatment with dilute sulfuric acid to protonate the carboxylate groups. The use of sulfuric acid had the advantage of allowing precipitation and removal by filtration of the sodium cations still present as Na_2SO_4.

We observed that the intermediate Pd−thiol particles did not remain in solution when methanol was used, although it has been reported that the use of methanol as a solvent allows successful synthesis of MUA-protected Au particles.[33]

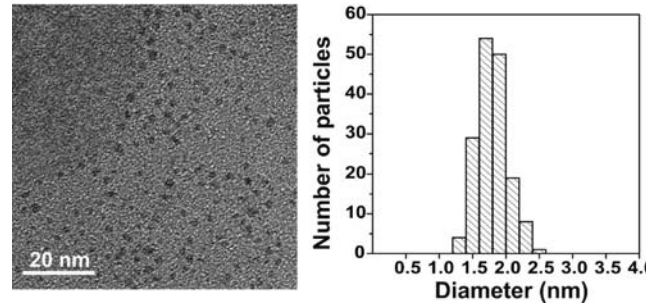

Figure 2. HRTEM (left) image of MUA-protected Pd nanoparticles together with the histogram of particle size distribution (right).

Representative HRTEM (Figure 2, left) and HAADF-STEM (Figure S1, Supporting Information) images of the as-synthesized protected Pd nanoparticles show the particles have an average metal core diameter of 1.8 nm and a very narrow dispersion ($\sigma = 0.2$ nm) (Figure 2, right).

^{1}H NMR data (Figure S2, Supporting Information) show that MUA is indeed bound to the Pd particles in the organic layer as indicated by the broadened ^{1}H signals.[28] The absence of the resonances attributable to the methylene protons next to sulfur is in accordance with the literature.[28] Small signals at about 3.50 and 3.60 ppm can be attributed to methylene groups next to an alcohol group. This suggests that some of the carboxylic acid has been reduced in a side-reaction; however, integration of the signals at 3.60 (or 3.50) and 2.30 ppm indicates that the extent of this reaction appears to be very low (<1%). Therefore, we conclude that most of the carboxylic groups are preserved under our experimental conditions.

The UV−visible profile (Figure S3, Supporting Information) shows a monotonic decay from 300 to 900 nm. There is no clear evidence of a surface plasmon (SP) band, although a band has been reported at 302 nm for 2.2 nm Pd nanoparticles protected with octadecanethiol.[34]

FT-IR spectra of both free MUA and MUA-Pd nanoparticles are reported in Figure S4 (Supporting Information). The IR spectrum of free MUA shows the presence of the S−H stretching frequency at about 2600 cm^{-1}. This band vanishes in the IR spectrum of Pd nanoparticles, suggesting that MUA is bound to the nanoparticles through a Pd−S bond. Furthermore, there is a small shift in the position of the carbonyl

(32) Chen, S.; Kimura, K. *Langmuir* **1999**, *15*, 1075.

(33) Laaksonen, T.; Ahonen, P.; Johans, C.; Kontturi, K. *ChemPhysChem* **2006**, *7*, 2143.

(34) Yee, C. K.; Jordan, R.; Ulman, A.; White, H.; King, A.; Rafailovich, M.; Sokolov, J. *Langmuir* **1999**, *15*, 3486.

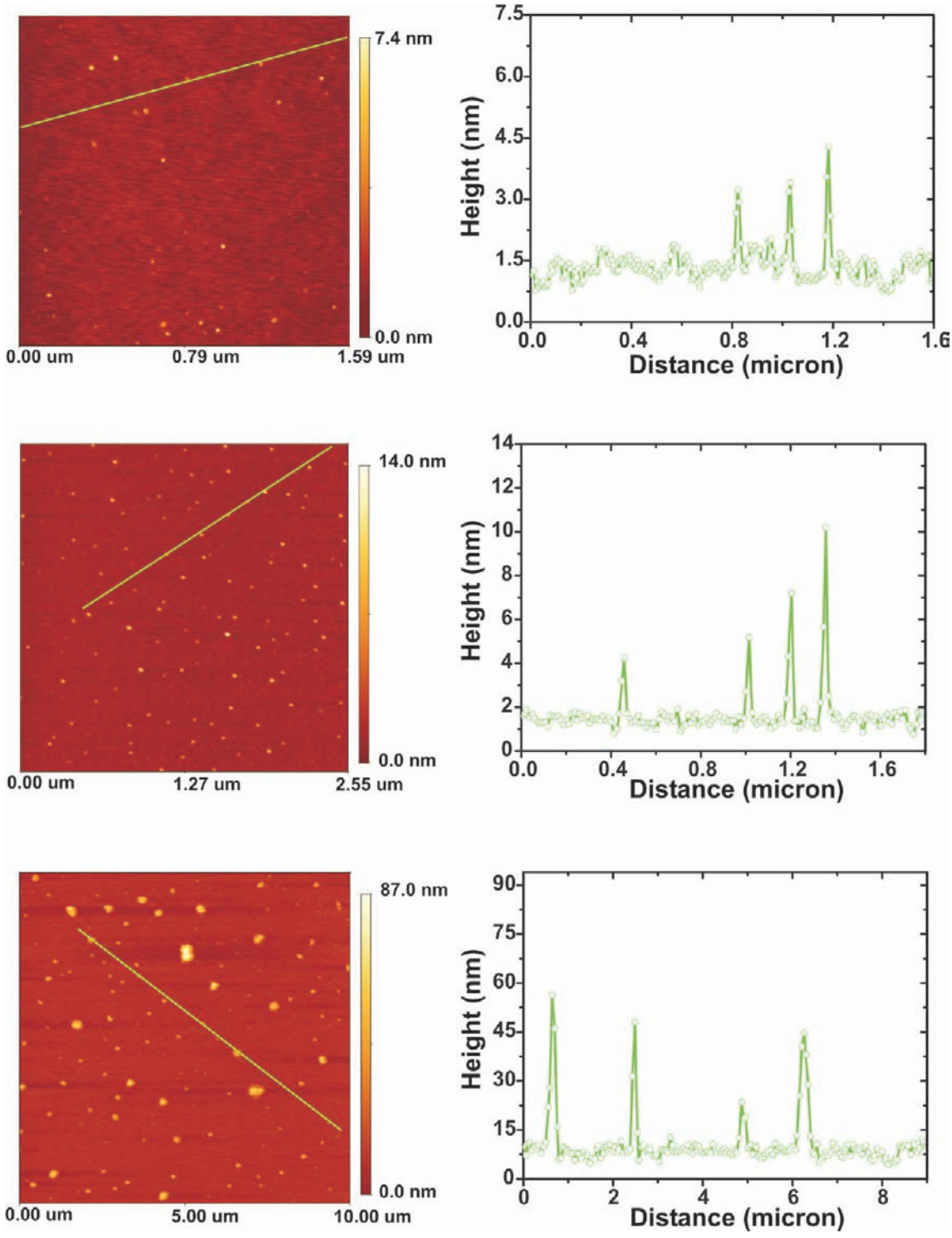

Figure 3. AFM images of MUA-Pd nanoparticles (top), Pd−Ce alkoxide assemblies (center), and dispersible Pd@CeO_2 core−shell nanostructures (bottom) together with line-height measurements.

stretching band from 1698 cm^{-1} (free MUA) to 1714 cm^{-1} (MUA-Pd nanoparticles). The peak shift is in accordance with reports on MUA-protected Au nanoparticles.[27] Some features of the spectrum are not due to MUA-Pd particles: the band at 1610 cm^{-1} (assigned to water), the sharp band at 1385 cm^{-1} (assigned to Na^+ impurities in the KBr[35]), and the broad band between 1300 and 1000 cm^{-1} (assigned to sulfates still present[36]).

3.3. Agglomeration of MUA-Pd Nanoparticles. The agglomeration of particles with carboxylic groups on the surface of the monolayer has been discussed in the literature. Intermolecular hydrogen bonding between protonated carboxylic groups on different particles has been reported as cause of the agglomeration.[37−40] However, when metal cations are present in solution, the metal-ion coordination chemistry of carboxylates becomes the driving force for agglomeration. This property has

been extensively used to prepare films of nanoparticles onto glass substrates,[41] for the detection of metal ions,[42−45] and for the investigation of metal-to-metal nanoparticle electron transfer chemistry.[46] Laaksonen et al. prepared MUA-Au nanoparticles and observed that precipitation depended on the size of the cations in solution.[33]

The presence of metal ions during our synthesis is consistent with a scenario in which agglomeration is induced by the coordination of metal ions to the carboxylic groups. The addition of $NaBH_4$ leads to an increase in the pH to a final value of 10 and to the precipitation of the particles. Agglomeration is reversible, because the particles redissolve at pH values lower than about 4.5. This value is close to the pK_a of mercaptoundecanoic acid. Furthermore, we observed that the addition of Fe(III), Ce(IV), or Ni(II) salts to acidic solution of MUA-Pd nanoparticles leads to a rapid agglomeration. Redissolution of the Pd particles could be achieved by sequestering the metal cations, through the addition of ethylendiamine tetraacetic acid (EDTA).

3.4. Self-Assembly of Cerium(IV) Alkoxide around MUA-Pd Nanoparticles. The second preparation step consists of the coupling reaction between cerium(IV) tetrakis(decyloxide), which is used as the ceria precursor, and the as-synthesized MUA-Pd nanoparticles. The reaction proceeds by exchange between an alkoxy group on the Ce precursor and carboxylic moieties on the surface of the Pd particles, the latter functionalities being stronger ligands then alkoxy groups.[47] As discussed earlier, the addition of "weakly coordinated" Ce(IV) cations (from $(NH_4)_2Ce(NO_3)_6$) to Pd-MUA nanoparticles results in agglomeration due to the formation of networks between the particles (vide supra). In contrast, the use of long-chain $Ce(OR)_4$ precursors allows for self-assembly of a Ce(IV) layer on the outside of the Pd particles without agglomeration, with the alkoxide tails providing the necessary steric repulsion to keep the particles well separated. However, to favor the assembly process with respect to the formation of networks/agglomerates, it was necessary to add the solution of Pd nanoparticles to cerium alkoxide solution slowly to ensure that the cerium(IV) alkoxide remain in excess. We observed that adding the cerium(IV) alkoxide to a solution of Pd particles caused the particles to agglomerate and then to precipitate out of solution. Presumably, with a deficit of alkoxide, carboxyls on different MUA-Pd particles can bind to the same Ce(IV) moiety, resulting in agglomeration.

It is worth noting that, although MUA-Pd particles are soluble in polar solvents such as methanol, ethanol, acetone, and tetrahydrofuran (THF), they are insoluble in dichloromethane and chloroform or other nonpolar solvents. Following reaction with the cerium(IV) alkoxide in THF, the product can be redissolved in nonpolar solvents such as hexane, giving indirect evidence that the carboxylic groups of the MUA-Pd particles have been successfully bound to cerium(IV) alkoxide.

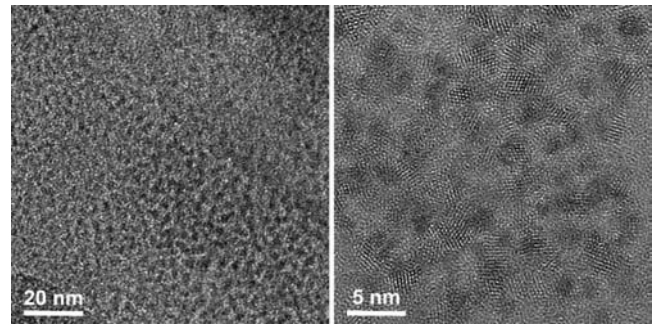

Figure 4. HRTEM images of dispersible Pd@CeO_2 nanostructures.

3.5. Controlled Hydrolysis To Obtain Dispersible Pd@CeO_2 Nanostructures. The subsequent addition of dodecanoic acid (1 mol with respect to Ce(IV)) caused the partial replacement of the alkoxy groups bound to Ce(IV). Dodecanoic acid serves two main purposes: to modulate hydrolysis of the cerium(IV) alkoxide and to confer solubility to the final product. The added dodecanoic acid is limited to 1 mol to preserve most of the alkoxy groups. Because the hydrolysis of carboxylate−cerium complexes is difficult and these compounds are stable in water,[48] using a large excess is undesirable. Sufficient dodecanoic acid is required to control the rates of hydrolysis and condensation and to allow for control over the growth of the ceria layer. Carboxylic acids are known to modify hydrolysis for alkoxides of other metals.[47] Furthermore, sufficient dodecanoic acid is required to confer solubility to the final product. The last step consists of the hydrolysis of the Pd−Ce system following treatment with dodecanoic acid, from which a hybrid organic−inorganic material composed of MUA-protected Pd nanoparticles and CeO_2 is obtained (Figure 1). By changing the amount of Ce alkoxide that is added to the particles, it is possible to obtain different concentrations of Pd (2.5, 10, or 50 wt %) and to tune the thickness of the CeO_2 layer around the particles.

The FT-IR spectrum of Pd(2.5 wt %)@CeO_2 indicates the presence of COO−Ce bonds (Figure S5, Supporting Information), with two strong bands located at 1530 and 1427 cm^{-1} that are typical for the stretching modes of chelated carboxylic groups bound to Ce.[49,50] This suggests that dodecanoic acid tails are still present in the nanostructures, and they determine the solubility of the final system in nonpolar solvents.

The effective removal of all coordinated alkoxy groups by washing with acetonitrile was confirmed by means of ^{1}H NMR (Figure S6, Supporting Information). The ^{1}H spectrum of Pd(2.5 wt %)@CeO_2 exhibits signals associated with dodecanoic acid tails only. Signals related to the MUA-Pd nanoparticle cores are not detectable due to their low concentration. Furthermore, the signal corresponding to the methylene group next to the carboxylic group is broadened into the baseline, and the other signals are markedly broadened as well, likely a result of the

(35) Goriletsky, V. I.; Mitichkin, A. I.; Belenko, L. E.; Rebrova, T. P. *Semicond. Phys., Quantum Electron. Optoelectron.* **2001**, *4*, 139.
(36) Gamo, I. *Bull. Chem. Soc. Jpn.* **1962**, *35*, 1058.
(37) Simard, J.; Briggs, C.; Boal, A. K.; Rotello, V. M. *Chem. Commun.* **2000**, 1943.
(38) Si, S.; Mandal, T. K. *Langmuir* **2006**, *23*, 190.
(39) Han, L.; Luo, J.; Kariuki, N. N.; Maye, M. M.; Jones, V. W.; Zhong, C. J. *Chem. Mater.* **2003**, *15*, 29.
(40) Sen, T.; Patra, A. *J. Phys. Chem. C* **2009**, *113*, 13125.
(41) Zamborini, F. P.; Hicks, J. F.; Murray, R. W. *J. Am. Chem. Soc.* **2000**, *122*, 4514.
(42) Yang, W.; Gooding, J. J.; He, Z.; Li, Q.; Chen, G. *J. Nanosci. Nanotechnol.* **2007**, *7*, 712.
(43) Kim, Y.; Johnson, R. C.; Hupp, J. T. *Nano Lett.* **2001**, *1*, 165.
(44) Si, S.; Raula, M.; Paira, T. K.; Mandal, T. K. *ChemPhysChem* **2008**, *9*, 1578.
(45) Slocik, J. M.; Zabinski, J.; Phillips, D. M.; Naik, R. R. *Small* **2008**, *4*, 548.
(46) Leopold, M. C.; Donkers, R. L.; Georganopoulou, D.; Fisher, M.; Zamborini, F. P.; Murray, R. W. *Faraday Discuss.* **2004**, *125*, 63.
(47) Urlaub, R.; Posset, U.; Thull, R. *J. Non-Cryst. Solids* **2000**, *265*, 276.
(48) Gradeff, P. S.; Schreiber, F. G.; Grosbois, J.; Mauermann, H. Ceric hydrocarbyloxy nitrates and their use in organic synthesis. U.S. Patent 4920204, 1990.
(49) Nguyen, T. D.; Do, T. O. *J. Phys. Chem. C* **2009**, *113*, 11204.
(50) Zhang, J.; Ohara, S.; Umetsu, M.; Naka, T.; Hatakeyama, Y.; Adschiri, T. *Adv. Mater.* **2007**, *19*, 203.

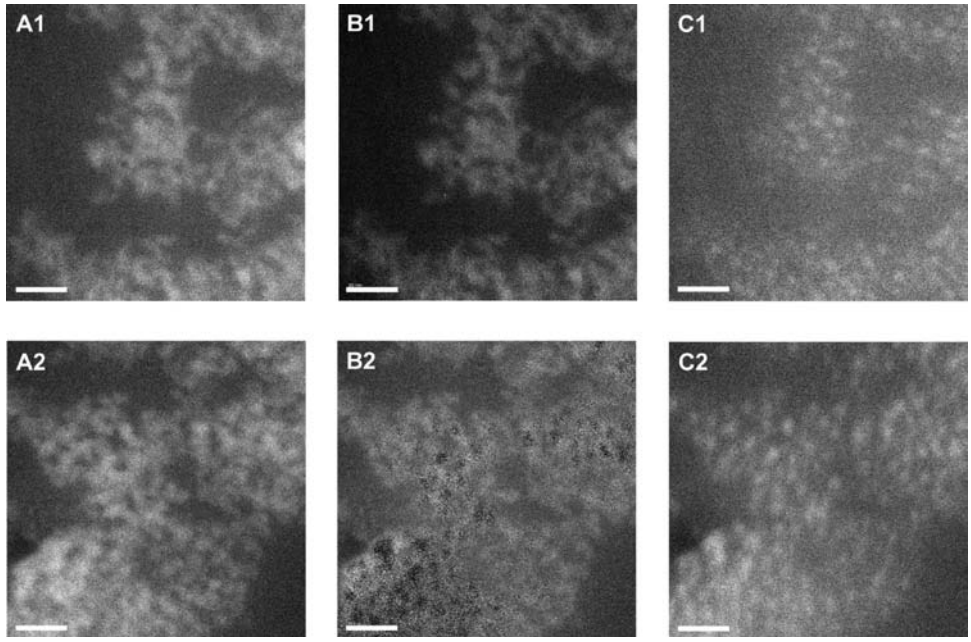

Figure 5. EELS maps of two different regions (denoted as 1 and 2) of dispersible Pd@CeO_2 nanostructures. Respectively: Ce postedge (A, all of the elements contribute to the image), Ce map (B, only Ce contributes), and Ce pre-edge (C, only Pd and S contribute). The scale bars represent 20 nm.

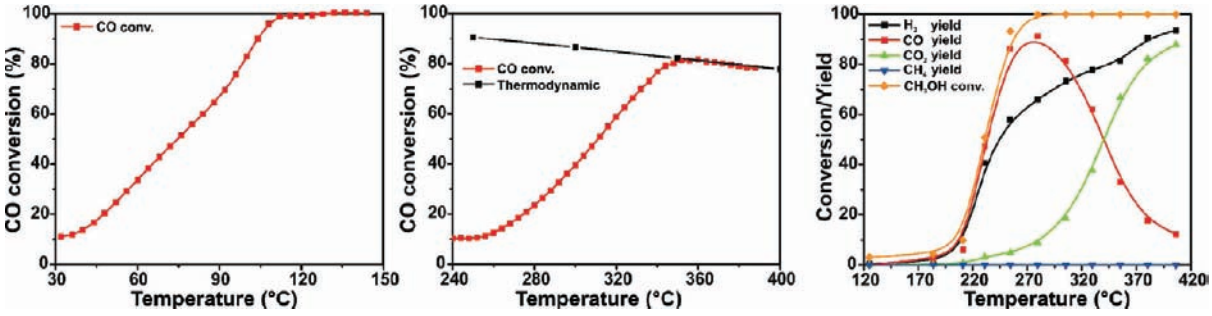

Figure 6. Catalytic activity of Pd(1%)@CeO_2(9%)/Al_2O_3, prepared from Pd@CeO_2 nanostructures, for CO oxidation (left), the water−gas shift (center), and methanol steam reforming (right) reactions.

slow mobility of these assemblies in solution and the formation of a hybrid organic−inorganic material.

The product is effectively dispersible in a range of solvents, from THF to hydrocarbons such as hexane, without any sign of aggregation. Moreover, it can be isolated after removing the solvent as an orange-brown oil and redissolved again.

3.6. Microscopy Characterization of Pd@CeO_2. The preparation of dispersible Pd@CeO_2 core−shell nanostructures has been demonstrated using AFM, TEM, and STEM.

Atomic Force Microscopy (AFM). AFM has proven to be a convenient means of following the development of Pd(2.5 wt %)@CeO_2 structures. Although resolution in the lateral (x, y) dimensions is limited by probe tip convolution,[51] nanoparticle heights (z dimension) can be effectively measured with subnanometer resolution. Unlike TEM, which is sensitive mainly to the metallic core, AFM is sensitive to the entire structure, consisting of both the Pd core and the organic ligands in the monolayer. Images were obtained in the tapping mode to avoid tip-induced particle mobility observed when contact-mode is employed.[52] The materials were analyzed starting from MUA-Pd nanoparticles (Figure 3, top), to the intermediate Pd−Ce alkoxide assembly (Figure 3, middle), to the final dispersible Pd@CeO_2 core−shell nanostructures (Figure 3, bottom). These results must be viewed as qualitative, because quantitative measurements would require further study on the tip−sample or sample−substrate interaction. The deposition of the structures onto the substrate was found to give reproducible results, and images on different regions of the sample that were taken gave reproducible height measurements.

On the basis of the AFM results, the starting MUA-Pd nanoparticles show an average height of about 3.0 nm. Taking into account the diameter of Pd core (about 1.8 nm) and the length of MUA chains (about 1.6 nm), a diameter of about 5.0 nm would be expected. However, height anomalies are known to occur for particles with dimensions less than 10 nm, and the discrepancy in our case could be attributed to tip−sample interactions,[53] a tilting angle of the chains in the monolayer,[54] or the flattening of the organic monolayer.[55] It is also possible

(51) Ramirez-Aguilar, K. A.; Rowlen, K. L. *Langmuir* **1998**, *14*, 2562.

(52) Junno, T.; Anand, S.; Deppert, K.; Montelius, L.; Samuelson, L. *Appl. Phys. Lett.* **1995**, *66*, 3295.

(53) Ebenstein, Y.; Nahum, E.; Banin, U. *Nano Lett.* **2002**, *2*, 945.

(54) Yu, J. J.; Ngunjiri, J. N.; Kelley, A. T.; Garno, J. C. *Langmuir* **2008**, *24*, 11661.

(55) Gu, Y.; Xie, H.; Gao, J.; Liu, D.; Williams, C. T.; Murphy, C. J.; Ploehn, H. J. *Langmuir* **2005**, *21*, 3122.

that the entire organic monolayer does not survive in the deposition process.

When the particles are reacted with Ce(IV) alkoxide, the average particle height increases to about 5.0 nm. This difference agrees with the expected increase in the diameter of the assemblies due to the presence of the alkoxide tails. The expected increase in particle diameter would be 3.2 nm, but the diameter is again lower, likely for the same reasons discussed above.

Following hydrolysis to obtain the dispersible Pd@CeO_2 nanostructures, the size of the particles increased to an average of approximately 30 nm. In this case, some larger aggregates (up to ca. 90 nm) are present as well; these are probably agglomerates of more than one discrete particle. Assuming that the dodecanoic acid chains contribute to the overall diameter of the system by 3.2 nm, the AFM results would suggest formation of a CeO_2 shell about 11 nm thick. Using the densities of CeO_2 and metallic Pd, the size of the MUA-Pd core (3.0 nm), and assuming a spherical Pd core and CeO_2 shell, we estimate that the shell thickness should be approximately 2.5 nm for Pd@CeO_2 nanostructures that are 2.5 wt % Pd and 97.5 wt % CeO_2, if the ceria layer were dense. We suggest that the Pd@CeO_2 particles are much larger than this because the Pd@CeO_2 nanostructures are highly porous, with the ceria layer being composed of small ceria crystallites. Indeed, catalytic data that will be discussed later indirectly confirm the porous nature of the ceria layer and the accessibility of the Pd surface to reactive molecules.

Electron Microscopy (TEM and STEM). Pd@CeO_2 nanostructures were also characterized using TEM and STEM techniques. Because of the high electron density of CeO_2, imaging metals on this support can be difficult,[56] and this problem is exacerbated when the metal is fully surrounded by CeO_2. Therefore, to facilitate the visualization of Pd cores, we prepared Pd@CeO_2 nanostructures with a lower ceria layer thickness (ceria from 97.5 to 50 wt %). Nevertheless, high-resolution TEM (HRTEM) images show only crystallites with lattice spacing of 0.33 nm (Figure 4), in agreement with the (111) lattice spacing of CeO_2. It should be noted that, despite the fact that the lattice spacing is in accordance with the formation of CeO_2, we cannot rule out that at least a fraction of the material is composed by a mixture of CeO_2 and cerium oxy-hydroxy complexes. However, HRTEM characterization suggests that, if this occurs, most of the material is composed by nanocrystalline CeO_2. STEM images with associated energy dispersive X-ray analysis (EDS) (Supporting Information, Figure S7) show individual particles having the correct Pd, S, Ce, and O compositions. Because electron energy loss spectroscopy (EELS), in association with STEM, can differentiate compositions in core−shell structures,[57] we obtained similar images using an EELS filter to distinguish the elemental contributions, with representative results shown in Figure 5 (regions 1 and 2). Figure 5A shows images obtained at the Ce postedge, where all of the elements (Ce, Pd and S) contribute to the final micrographs. The contributions from lighter elements, such as C and O, are limited due to their very low scattering factors. Removing the pre-edge contribution (mainly Pd and S) from the total postedge signals (Ce, Pd, and S) gives a map of the Ce distribution (Figures 5B), which is very similar to Figure 5A. Collecting the signals from the Ce pre-edge, which removes the Ce contribution from the image, results in Figures 5C. Individual particles having Pd and S are clearly visible, corresponding to the metallic cores. This is consistent with a Ce-containing layer surrounding the Pd particles and demonstrates the core−shell nature of the nanostructures.

3.7. Accessibility of Palladium Phase in the Pd@CeO_2 Nanostructures. To highlight the accessibility of the Pd and the potential of this Pd@CeO_2 precursor for the preparation of heterogeneous catalysts, we impregnated the Pd@CeO_2 core−shell nanostructures onto a high surface area, thermally stable support (Al_2O_3). CO oxidation, the water−gas shift (WGS), and methanol steam reforming reactions were then used to test accessibility and activity. As shown in Figure 6, the present systems show promising, even if not optimized, activity for each of the reactions. Furthermore, the catalysts exhibited significant CO uptake, corresponding to 11% Pd apparent dispersion. All of these observations demonstrate that the Pd is accessible to CO, water, oxygen, and even methanol, implying again that the ceria shell must be porous.

4. Conclusions

We successfully prepared dispersible Pd@CeO_2 core−shell nanostructures by exploiting the self-assembly between functionalized Pd nanoparticles and cerium(IV) alkoxides. The Pd@CeO_2 core−shell nanostructures are effectively dispersible in a range of organic solvents without any sign of agglomeration. We demonstrated that the dimension of the metal core and the thickness of the oxide layer can be tuned and that the metal phase is accessible, because these nanostructures are interesting precursors for the preparation of active heterogeneous catalysts.

Acknowledgment. Professors Mauro Graziani and Lucia Pasquato (University of Trieste) are acknowledged for stimulating helpful discussions. M.C. thanks the U.S. Air Force for a fellowship. R.J.G. and N.L.W. acknowledge support from AFOSR (MURI), Grant No. FA9550-08-1-0309. M.C., T.M., and P.F. acknowledge the University of Trieste, ICCOM-CNR, INSTM, and PRIN2007 "Sustainable processes of 2nd generation for the production of H_2 from renewable resources" for financial support. The assistance of Dr. Shiwoo Lee and Dr. Douglas Yates is gratefully acknowledged, as is the use of the PENN Regional Nanotechnology Facility.

Supporting Information Available: Representative HAADF-STEM image, ^{1}H NMR, UV−visible, and FT-IR spectra of MUA-protected Pd nanoparticles; ^{1}H NMR and FT-IR spectra of dispersible Pd(2.5 wt %)@CeO_2 core−shell nanostructures; representative STEM image and associated EDS scan of dispersible Pd(50 wt %)@CeO_2 core−shell nanostructures; and calculations of conversions and yields in CO oxidation, WGS, and methanol steam reforming reactions. This material is available free of charge via the Internet at http://pubs.acs.org.

JA909131K

(56) González, J.; Hernández, J. C.; López-Haro, M.; del Río, E.; Delgado, J. J.; Hungría, A. B.; Trasobares, S.; Bernal, S.; Midgley, P. A.; Calvino, J. J. *Angew. Chem., Int. Ed.* **2009**, *48*, 5313.

(57) Catala, L.; Brinzei, D.; Prado, Y.; Gloter, A.; Stéphan, O.; Rogez, G.; Mallah, T. *Angew. Chem., Int. Ed.* **2009**, *48*, 183.